20120038A

厚生労働科学研究費補助金

創薬基盤推進研究事業

アジア人種型２型糖尿病の治療法及び治療薬の開発を可能にするマウス及びヒト膵β細胞由来のモデル細胞系の構築

平成24年度　総括研究報告書

研究代表者　魏　范研

平成 25（2013）年　5 月

目　　次

厚生労働科学研究費補助金（創薬基盤推進研究事業）

総括研究報告書

アジア人種型２型糖尿病の治療法及び治療薬の開発を可能にするマウス及びヒト膵β細胞由来のモデル細胞系の構築

研究代表者　魏　范研　熊本大学　助教

研究要旨

アジア型２型糖尿病は、非肥満及び低インスリン分泌といった特徴を持ち、欧米型２型糖尿病とは異なる病態を示す。一方、既存の糖尿病治療薬は、特にアジア人種において高頻度の副作用が報告されている。従って、アジア人種に適した新規治療薬及び治療法の開発が必要である。しかし、アジア型２型糖尿病の発症原因が不明であったため、治療薬の開発及び評価が不可能であった。

Cdkal1 遺伝子の一塩基多型変異(SNPs)は、アジア人種において約四人に一人という高い頻度で保有されており、アジア型２型糖尿病の原因遺伝子の一つである。Cdkal1 は、リジン tRNA をチオメチル化し、リジンコドンの正確な翻訳に必要であった。また、Cdkal1 の膵臓β細胞欠損マウス(Cdkal1 KO)マウスでは、プロインスリンのリジンコドンにおける誤翻訳が原因となり、低インスリン分泌及び非肥満といったアジア型２型糖尿病に類似した表現型を呈した。さらに、２型糖尿病発症と相関する危険型 Cdkal1 SNPs を有する人において Cdkal1 の特異的な転写産物の発現量が低下し、Cdkal1 活性が低下していた。以上のことから、Cdkal1 遺伝子変異を伴うアジア型２型糖尿病の発症は、Cdkal1 活性低下による tRNA 修飾異常ならびにリジンコドンの誤翻訳に起因すると明らかになった。

本研究では、Cdkal1 KO マウス由来の Cdkal1 欠損膵β細胞株、また、危険型 Cdkal1 SNPs を有するヒト Fibroblast 由来の iPS 細胞から分化誘導したヒト膵β細胞を利用して、アジア型２型糖尿病の特徴を有する細胞評価系を構築することを目的とする（２４年度)。また、既存の治療薬や独自の低分子化合物ライブラリーを利用し、Cdkal1 遺伝子変異に伴うアジア型２型糖尿病治療薬の評価及び新規開発にも着手する（２５年度)。

本研究成果により、世界初の Cdkal1 遺伝子変異に起因するアジア型２型糖尿病の特徴を有するマウス及びヒト膵β細胞のモデル系の確立が期待され、Cdkal1 遺伝子変異を有する２型糖尿病に対する最適な治療薬及び治療法を確立することが可能となる。

厚生労働科学研究費補助金（創薬基盤推進研究事業）

総括研究報告書

国立大学法人　熊本大学
大学院生命科学研究部　助教
魏　范研

A．研究目的

日本における２型糖尿病患者は、その予備軍も含めると現在1,370万人と推定されており（厚生労働省実態調査より）、年々患者数は増加している。また近年中国やインドでも経済の発展に伴い、患者数が激増しており、アジア地域における糖尿病の治療法の確立は社会的な要請が高い。

２型糖尿病に対する治療薬は、既に多く開発され、広く一般使用されている。しかし、これらの治療薬は人種間の体質差及び病態差を考慮に入れて開発されたものではない。そのため、同様な治療薬を用いても、日本における重症低血糖発見率は米国食品医薬品局データベースのデータに比べて 1,000 倍以上と高率である（Medical Tribune, Vol. 44. No. 47）。この事実が示すように、現在の治療薬や治療法は、必ずしも日本人を含むアジア人種にとって最適なものではない。従って、アジア人種に適した治療法や新規治療薬の開発が必要である。しかし、なぜ欧米人種とアジア人種に２型糖尿病の病態差が生じるか、その分子機構は不明であったため、アジア型２型糖尿病に対する治療法や新規治療薬を開発するための基盤が存在しなかった。

我々は世界に先駆けてCdkal1の分子機能を明らかにし、アジア２型糖尿病発症の分子機構の一端を明らかにした。そこで、我々独自の研究成果に基づき、本研究においてアジア型２型糖尿病に対する治療法及び治療薬の開発を可能にするマウス及びヒト膵β細胞由来のモデル細胞系の構築を目的とし、研究を行った。

B．研究方法

項目①　誤翻訳を検出するCdkal1 KO マウス膵β細胞由来の細胞アレイの作製

1. 誤翻訳検出用レポーターウィルスの作製

Firefly ルシフェラーゼの 529 番のリジンは、ルシフェラーゼの活性に非常に重要であるため、そのリジンコドンが他のアミノ酸コドンに改変されると、ルシフェラーゼ活性はほぼ消失する。即ち、Firefly ルシフェラーゼ活性は、529 番のリジンの翻訳精度に強く依存する。一方、Renilla ルシフェラーゼ活性はリジンに依存しない。本研究では、Firefly ルシフェラーゼと Renilla ルシフェラーゼを連結させたレポーターを含むレンチウィルスをまず作製する。

2. レポーターを含むCdkal1 KOβ細胞由来のスクリーニング系の構築

誤翻訳を検出するレポーターを含むウィルスを Cdkal1 KOβ細胞株に導入した後、96-well プレートにβ細胞株を生着させる。90%以上の生存率でマルチウェルに生着することを目標とする。なお、Cdkal1 遺伝子欠損β細胞株は、我々が現有するCdkal1 KOマウス（特願 2009-258382）の膵β細胞を SV40 Large T 抗原の導入によって不死化させたも

のである。ルシフェラーゼ活性は、細胞を融解させた後、ATP による発光効果を利用した市販のキットを用いて測定する。

項目②　Cdkal1 SNPs を有するヒト膵β細胞由来のスクリーニング系の構築

1. Fibroblast から iPS 細胞の誘導

健常人 Fibroblast における Cdkal1 遺伝子型を PCR により同定した後、危険型 Cdkal1 SNPs 並びに非危険型 Cdkal1 SNPs を有する Fibroblast に、SOX2、Klf4、Oct3/4、c-Myc を導入し、iPS 細胞を作製する。

2. iPS 細胞からβ細胞への誘導

iPS 細胞からβ細胞への誘導は、我々が独自に開発し、特許出願した関連技術を用いる（特願2011-071530）。本技術は特殊なコーティング剤を用いて高効率で iPS から膵β細胞に誘導できるものである。本研究では、この技術を応用して、PDX-1、NeuroD、MafA タンパクを iPS 細胞に導入することにより膵β細胞を作製する。誘導結果は、インスリン遺伝子の発現量をリアルタイム PCR によって測定し、検討する。なお、PDX-1,NeuroD 及び MafA タンパクを細胞に導入する際、我々の研究グループが持つタンパク導入法技術を利用する（PCT / JP2003 / 012816 (W02004/032955)）.

項目③　低分子化合物のスクリーニング

1. 低分子化合物による一次スクリーニング

項目①及び項目②で作製した細胞アレイに既存の糖尿治療薬或は低分子化合物ライブラリーを加え、ルシフェラーゼ活性を測定することにより、治療薬あるいは低分子化合物の誤翻訳改善効果を評価する。抗糖尿病薬は、スルフォニル尿素系薬（グリベンクラミド）、GLP-1 に対する治療薬（Exendin-4 や DPP4 阻害剤）、ビグアナイド系薬（メトホルミン）を予定している。低分子化合物ライブラリーはすでに現有するものを用いる。一次スクリーニングにおいて翻訳精度を改善した低分子化合物を一次陽性化合物とする。

2. 二次スクリーニング

次に、低グルコース培地で培養中の同細胞アレイに一次陽性化合物を加え、１５分後に化合物を含む高グルコース培地を置換して刺激する。インスリンが分泌されるには細胞内カルシウム濃度の上昇が重要であるため、刺激時の培地中に分泌されるインスリンの量及び細胞内カルシウムの上昇を測定する。化合物を加えない細胞を対照とし、化合物を加えた細胞においてインスリン分泌量あるいはカルシウム濃度が 1.5 倍以上に上昇した化合物を二次陽性化合物とする。二次陽性化合物をさらに項目②で作製したヒト膵β細胞アレイに加え、誤翻訳及びインスリン分泌促進効果を評価する。

（倫理面への配慮）

本研究は，患者もしくは患者からの得られたサンプルを使用するような臨床研究、臨床疫学研究では無い。本研究で計画されているヒ

ト細胞での遺伝子解析研究はすでに学内倫理委員会によって承認されている（ゲノム第１５９号）。

組換えDNA実験は、本大学の遺伝子組換え生物等第二種使用等安全委員会の承認受けた後、使用する微生物のレベルに応じた実験室で行なう。また、研究開発の過程で使用する遺伝子組み換え生物（ウィルス等）はすべて倫理委員会から承認されている（承認番号21-075）。

ヒトiPS細胞の使用に関しては、「ヒトES細胞の樹立及び使用に関する指針」を遵守し、本大学のヒトES細胞研究倫理委員会の承認を受けた後、研究を実施する。

C．研究結果

①誤翻訳を検出するルシフェラーゼを用いたレポーターをレンチウィルスに組み込み、HEK293細胞にて大量にウィルスを作製した。次に、Cdkal1 KOマウスとSV40を発現するトランスジェニックマウスを交配させることにより得られたCdkal1を欠損した不死化膵β細胞に、レポーターを含むレンチウィルスを導入した。その後、β細胞を９６ウェルプレートに生着させ、細胞アレイを作製した。細胞の生着率は９０％以上に達したことを確認した後、ルシフェラーゼ検出試薬を用いて、Renilla luciferase及びFirefly luciferaseの発光強度を測定した。その結果、Firefly luciferaseの発光強度は312115カウント、Renilla luciferaseの発光強度は657488カウントと測定可能範囲内の発光強度を得ることが出来た。

②PCR法により遺伝子型を確かめられた危険型Cdkal1 SNPsを有するヒトFibroblastにSOX2、Klf4、Oct3/4、c-Mycを有するセンダイウィルスを導入し、iPS細胞を作製した。その後、iPS細胞を804G細胞の分泌液をコーティングしたプレートに生着させ、細胞透過ドメインを有するPDX-1、NeuroD、MafAタンパクを直接iPS細胞に加えた。誘導後１７日目に、定量PCR法により内在性pdx1やインスリン遺伝子の発現を検出した。

③Cdkal1 KOマウス由来の細胞アレイ（①において実施済み）に低分子化合物を加え、翻訳精度によるスクリーニングを行った。その結果１７種類の化合物において翻訳精度の向上効果が見られた。さらにこれらの化合物を細胞内カルシウム及び培養上清中のインスリン分泌量で二次スクリーニングを行った結果、８種類の化合物が陽性反応を示した。

D. 考察

以上の結果から、本研究の申請時における研究目的の一つであるマウス由来のスクリーニング系の構築を達成したと考える。また、今年度において危険型SNPを有するヒト繊維芽細胞から膵β細胞の分化誘導にすでに成功している。翻訳異常を検出するレポーターウィルスを感染させれば、ヒト膵β細胞由来のスクリーニング系を完成させることができる。一方、前倒して実施したスクリーニングにより、翻訳精度及びインスリン分泌を向上

させる低分子化合物が発見された。これらの化合物の抗糖尿病効果を動物個体においても確かめることができれば、アジア２型糖尿病に対する治療薬の開発という本研究の当初の目的を達成できると考える。一方、本スクリーニング系及び同スクリーニング系で発見した陽性化合物は、これまでにない効能をもつため、特許申請を行うと同時に、本学の専門部署を介して製薬企業などに技術移転を打診する。

E. 結論

平成２４年度の研究においてアジア型糖尿病の原因遺伝子及びその表現型を持つ Cdkal1 欠損マウス由来のスクリーニング系を構築した。また、同スクリーニング系を用いて小規模のスクリーニングを行った結果、翻訳精度を向上させながら、インスリン分泌を促進する低分子化合物の発見に至った。一方、２型糖尿病発症リスクが高い Cdkal1 遺伝子変異を有するヒト繊維芽細胞から iPS 細胞を作製し、さらにβ細胞へと分化誘導を行い、インスリン遺伝子を発現するβ細胞を得た。

F． 健康危険情報

本開発においてウィルスなどを用いたが、健康に危険を及ぼすことはなかった。

G． 研究発表

1. 論文発表

(1) Ueda Y, Wei FY, Hide T, Michiue H, Takayama K, Kaitsuka T, Nakamura H, Makino K, Kuratsu J, Futaki S, Tomizawa K. Induction of autophagic cell death of glioma-initiating cells by cell-penetrating D-isomer peptides consisting of Pas and the p53 C-terminus. Biomaterials. 2012 Dec;33(35):9061-9.

(2) Sato Y, Hatta M, Karim MF, Sawa T, Wei FY, Sato S, Magnuson MA, Gonzalez FJ, Tomizawa K, Akaike T, Yoshizawa T, Yamagata K. Anks4b, a novel target of HNF4α protein, interacts with GRP78 protein and regulates endoplasmic reticulum stress-induced apoptosis in pancreatic β-cells. J Biol Chem. 2012 Jun 29;287(27):23236-45.

(3) Okimoto N, Bosch OJ, Slattery DA, Pflaum K, Matsushita H, Wei FY, Ohmori M, Nishiki T, Ohmori I, Hiramatsu Y, Matsui H, Neumann ID, Tomizawa K. RGS2 mediates the anxiolytic effect of oxytocin. Brain Res. 2012 May 9;1453:26-33.

2. 学会発表

(1) 第９０回日本生理学会、東京
翻訳精度維持におけるｔＲＮＡ修飾の役割及びその破綻による病態の解析（口頭発表）

H. 知的財産権の出願・登録状況
（予定を含む。）

1. 特許取得（出願）

厚生労働科学研究費補助金（創薬基盤推進研究事業）

総括研究報告書

(1) 特願 2013- 47278 出願日：平成２５年３月８日 発明名称：ＲＮＡ修飾の簡易検出法、及び該検出法を用いた２型糖尿病の検査方法 (2) 特願 2013- 072391 出願日：平成２５年３月２９日 発明名称：２型糖尿病治療剤	

研究成果の刊行に関する一覧表

発表者氏名	論文タイトル名	発表誌名	巻号	ページ	出版年
Ueda Y, Wei FY, Hide T, Michiue H, Takayama K, Kaitsuka T, Nakamura H, Makino K, Kuratsu J, Futaki S, Tomizawa K.	D-isomer peptides consisting of Pas and the p53 C-terminus.	Biomaterials.	33	9061-9069.	2012
Sato Y, Hatta M, Karim MF, Sawa T, Wei FY, Sato S, Magnuson MA, Gonzalez FJ, Tomizawa K, Akaike T, Yoshizawa T, Yamagata K.	Anks4b, a novel target of HNF4α protein, interacts with GRP78 protein and regulates endoplasmic reticulum stress-induced apoptosis in pancreatic β-cells.	J Biol Chem.	287	23236-23245	2012
Okimoto N, Bosch OJ, Slattery DA, Pflaum K, Matsushita H, Wei FY, Ohmori M, Nishiki T, Ohmori I, Hiramatsu Y, Matsui H, Neumann ID, Tomizawa K.	RGS2 mediates the anxiolytic effect of oxytocin.	Brain Res.	1453	26-33	2012

Biomaterials 33 (2012) 9061–9069

Contents lists available at SciVerse ScienceDirect

Biomaterials

journal homepage: www.elsevier.com/locate/biomaterials

Induction of autophagic cell death of glioma-initiating cells by cell-penetrating D-isomer peptides consisting of Pas and the p53 C-terminus

Yutaka Ueda [a,b], Fan-Yan Wei [a], Taku-ichiro Hide [b], Hiroyuki Michiue [c], Kentaro Takayama [d], Taku Kaitsuka [a], Hideo Nakamura [b], Keishi Makino [b], Jun-ichi Kuratsu [b], Shiroh Futaki [d], Kazuhito Tomizawa [a,*]

[a] Department of Molecular Physiology, Faculty of Life Sciences, Kumamoto University, 1-1-1 Honjyo, Chuo-ku, Kumamoto 860-8556, Japan
[b] Department of Neurosurgery, Faculty of Life Sciences, Kumamoto University, 1-1-1 Honjyo, Chuo-ku, Kumamoto 860-8556, Japan
[c] Department of Physiology, Okayama University Graduate School of Medicine, Dentistry and Pharmaceutical Sciences, 2-5-1 Shikata-cho, Kita-ku, Okayama 700-8558, Japan
[d] Institute for Chemical Research, Kyoto University, Uji, Kyoto 611-0011, Japan

ARTICLE INFO

Article history:
Received 20 August 2012
Accepted 2 September 2012
Available online 21 September 2012

Keywords:
Brain
Peptide
Drug delivery
Apoptosis
Cell proliferation
Protein transduction

ABSTRACT

Glioblastoma multiforme (GBM) is the most aggressive and fatal brain tumor. GBM is resistant to chemotherapy and radiation. Recent studies have shown that glioma-initiating cells (GICs), which have characteristics of cancer stem cells, are responsible for the resistance to chemotherapy and radiation and regrowth. No effective therapy for GICs has been developed. Here we showed that D-isomer peptides (dPasFHV-p53C′) consisting of a cell-penetrating peptide (FHV), penetration accelerating sequence (Pas) and C-terminus of p53 (p53C′) induced the cell death of GICs. dPasFHV-p53C′ was effectively transduced into human GICs. The peptides dose-dependently inhibited cell growth and at 3 μM completely blocked the growth of GICs but not embryonic stem cells. Autophagic cell death was observed in the GICs treated with dPasFHV-p53C′ but apoptosis was not. dPasFHV without p53C′ showed the same effect as dPasFHV-p53C′, suggesting Pas to play a critical role in the cell death of GICs. Finally, dPasFHV-p53C′ reduced tumor mass in mice transplanted with GICs. Peptide transduction therapy using dPasFHV-p53C′ could be a new method for the treatment of GBM.

1. Introduction

Glioblastoma multiforme (GBM) is one of the most aggressive human tumors with a poor prognosis. The median survival of patients with GBM is less than 1 year, mainly because conventional postsurgical chemotherapeutic agents and irradiation exhibit limited effects [1,2]. A small subpopulation of CD133-positive cells has been identified in specimens of GBM and called glioma-initiating cells (GICs) [3,4]. The cells express additional stem cell markers, exhibit self-renewal and differentiation into glial and neuronal lineages, and can initiate xenograft tumors [5,6]. GICs are the only cell population with tumorigenic capacity in GBM and may possess innate resistance mechanisms against radiation- and chemotherapy-induced cell death, allowing them to survive and initiate tumor recurrence [7]. New approaches to GICs are needed for the treatment of GBM.

The C-terminus of p53 (p53C′), a biologically active tumor suppressor protein, is a lysine-rich domain subject to a variety of posttranslational modifications [8,9]. A peptide derived from the C-terminus activates specific DNA-binding by p53 *in vitro* through an unknown mechanism [10] and functions as a potent anticancer peptide [11]. Intracellular protein delivery using membrane-permeable peptide vectors has received increasing attention as a highly efficient way to modify cellular functions with therapeutic potential [12–14]. The vectors are often referred to as cell-penetrating peptides (CPPs) or protein transduction domain (PTD) peptides. Through conjugation with a short peptide vector (<12 amino acid residues) such as the PTD of the human immunodeficiency virus type 1 TAT protein (TAT), poly-arginine, and the PTD derived from flock house virus (FHV), various proteins have been introduced into cells and have successfully exerted their functions [12–14]. Previous studies have shown that D-isomer retro-inverso peptides consisting of p53C′ and TAT, which display greater stability, induce the apoptosis of cancer cells and significantly increase lifespan in animal models of terminal peritoneal carcinomatosis and peritoneal lymphoma expressing wild-type p53

* Corresponding author. Tel.: +81 96 373 5050; fax: +81 96 373 5052.
E-mail address: tomikt@kumamoto-u.ac.jp (K. Tomizawa).

0142-9612/$ – see front matter © 2012 Elsevier Ltd. All rights reserved.
http://dx.doi.org/10.1016/j.biomaterials.2012.09.003

[11,15]. However, a high concentration of the peptides is needed for the growth inhibition of cancer cells because the transduced peptides are mostly entrapped in macropinosomes, and then carried and degraded in lysosomes fused with macropinosomes [16].

Cathepsin D is a lysosomal enzyme that can cleave peptide segments such as KPILFFRLK [17]. We recently found that a retro sequence peptide of the cathepsin D-cleavable sequence (FFLIPKG) called the penetration accelerating sequence (Pas), enhanced the efficiency of intracellular delivery of bioactive peptides using

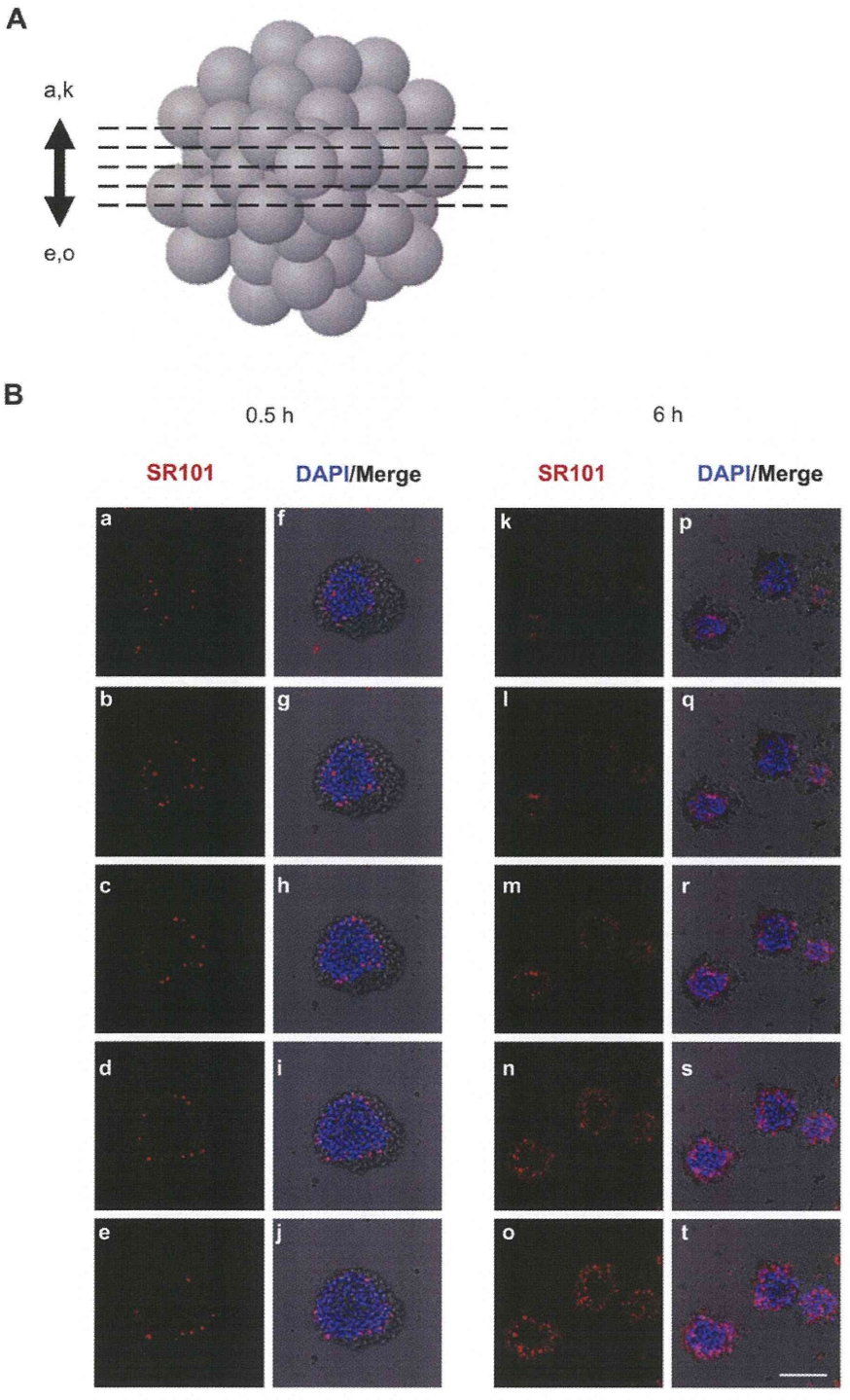

Fig. 1. Delivery of dPasFHV-p53C′-SR101 into human GICs. (A) Scheme of the images of serial optical sections in B. The images were multiple optical 4-μm step sections scanning the Z-dimension of laser scans of the sphere of GICs. (B) GICs that formed spheres were incubated with 10 μM dPasFHV-p53C′-SR101 for 0.5 and 6 h. After washing with PBS, SR101 signals (red) were observed with a laser confocal microscope. All nuclei were stained with DAPI (blue). Scale bar = 100 μm.

arginine-rich CPPs by breaking the macropinosomal membrane [18]. Moreover, the D-isomer peptides of p53C′ fused with the PTD of FHV and Pas (dPasFHV-p53C′) more significantly inhibited the growth of human glioma and bladder cancer cells, and induced apoptosis [18,19]. These results led us to believe that dPasFHV-p53C′ may be a tool for GBM therapy. However, the effect of the peptides on GICs is unclear. We have established human GIC lines that not only retain the characteristics of neural stem cells, but also form GBM with their original pathological features when transplanted *in vivo* [20]. In the present study, we examined the effect of dPasFHV-p53C′ on human GICs.

2. Materials and methods

2.1. Peptide synthesis

All of the peptides used were chemically synthesized by Fmoc (9-fluorenylmethyloxycarbonyl) solid-phase peptide synthesis on a Rink amide resin as described previously [18]. Briefly, deprotection of the peptide and cleavage from the resin were achieved by treatment with a trifluoroacetic acid/ethanedithiol mixture (95:5) at room temperature for 3 h followed by reversed-phase high performance liquid chromatography (HPLC) purification. Fluorescent labeling of the peptides was conducted by treatment with sulforhodamine 101 (SR101) (Invitrogen, Carlsbad, CA) in a dimethylformamide (DMF)/methanol mixture (1:1) for 1.5 h followed by HPLC purification. The structure of the products was confirmed by matrix-assisted laser desorption ionization time-of-flight mass spectrometry (MALDI-TOF/MS).

The structure of each peptide was as follows

1. dPasFHV-p53C′:

FFLIPKGRRRRNRTRRNRRRVR-G-KKHRSTSQGKKSKLHSSHARSG-amide

2. dPasFHV-p53C′-SR101:

FFLIPKGRRRRNRTRRNRRRVR-G-KKHRSTSQGKKSKLHSSHARSGC(SR101)- amide

3. dPasFHV:

FFLIPKGRRRRNRTRRNRRRVR

4. D-p53C′ (control peptide):

KKHRSTSQGKKSKLHSSHARSG-amide

5. L-p53C′ (control peptide):

KKHRSTSQGKKSKLHSSHARSG-amide.

The Pas segment is highlighted by the dashed line. The D-amino acids are shown in italics. A Gly residue was inserted as a linker to connect the dPasFHV/dFHV and p53C′ segments.

2.2. Cell culture

2.2.1. Preparation of GICs

Primary human GBM samples were obtained with consent from patients diagnosed with GBM and underwent surgical resection in Kumamoto University Hospital according to the guidelines of the University's Research Ethics Committee. The study was approved by the Ethics Committee. GICs were isolated from the samples as described previously [21]. Briefly, tumor samples were washed twice

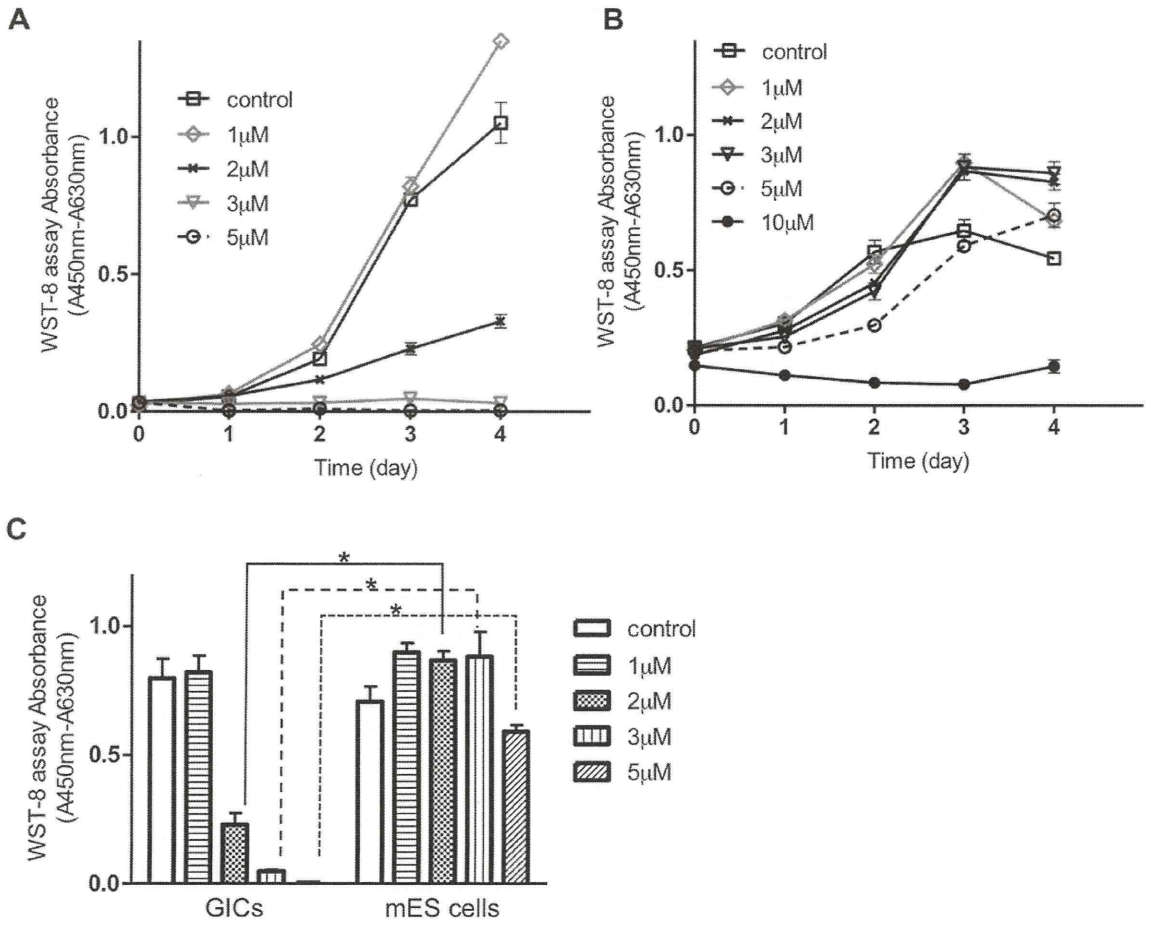

Fig. 2. Dose-dependent effect of dPasFHV-p53C′ on the growth of GICs (A) and mouse embryonic stem cells (B). Cells were incubated with each concentration of the peptide for the period indicated. As a control, cells were treated with 10 μM D-p53C′. The growth was evaluated with the WST-8 assay. (C) Comparison of the inhibitory effect of each concentration of peptide on the growth on day 4. $n = 4$ each. $^*P < 0.001$.

with PBS and dissociated with an enzymatic solution containing 0.25% Trypsin in 0.1 mM EDTA at 37 °C for 60 min. Dissociated cells were then cultured as tumor spheres in serum-free DMEM/F-12 (Invitrogen) containing human basic fibroblast growth factor (bFGF; 20 μM, Wako, Osaka, Japan), human epidermal growth factor (EGF; 20 μM, Peprotech, Rocky Hill, NJ), human leukemia inhibitory factor (LIF; 20 μM, Millipore, Billerica, MA), heparin (5 μM, Sigma–Aldrich, St. Louis, MO), insulin (10 μM, Sigma–Aldrich), N2 supplement (1%, Invitrogen) and B27 supplement (1%, Invitrogen) prior to use.

2.2.2. Mouse embryonic stem (ES) cells

The mouse ES cell line, ING112, containing a Ins1-promoter-driven GFP reporter transgene, was established by culturing blastocysts obtained from transgenic mice homozygous for the Ins1-GFP gene [22]. Cells were maintained on mouse embryonic fibroblast (MEF) feeders in Glasgow MEM supplemented with 1000 units/ml leukemia inhibitory factor (LIF), 15% Knockout Serum Replacement (KSR, Invitrogen), 1% fetal bovine serum (FBS), 100 μM nonessential amino acids (NEAA), 2 mM L-glutamine (L-Gln), 1 mM sodium pyruvate, 50 units/ml penicillin and 50 μg/ml streptomycin (P/S), and 100 μM β-mercaptoethanol (β-ME). MEFs lacking *Atg5* ($Atg5^{-/-}$ MEF) and wild-type MEFs ($Atg5^{+/+}$ MEF) were obtained from RIKEN CELL BANK (Tsukuba, Japan). The cells were maintained in DMEM (Invitrogen) supplemented with 10% fetal bovine serum (FBS) and 1% penicillin/streptomycin at 37 °C in 5% CO_2.

2.3. Cell viability assay (WST-8 assay)

Cell viability was determined using a WST-8 [2-(2-methoxy-4-nitrophenyl)-3-(4-nitrophenyl)-5-(2,4-disulfophenyl)-2H-tetrazolium] assay kit (Dojindo, Kumamoto, Japan). The sphere of GICs was dissociated into single cells using 0.02% EDTA. The cells were then seeded into 96-well plates and incubated with each concentration of peptide for the period indicated. Cell viability was measured every 24 h according to the manufacturer's instructions.

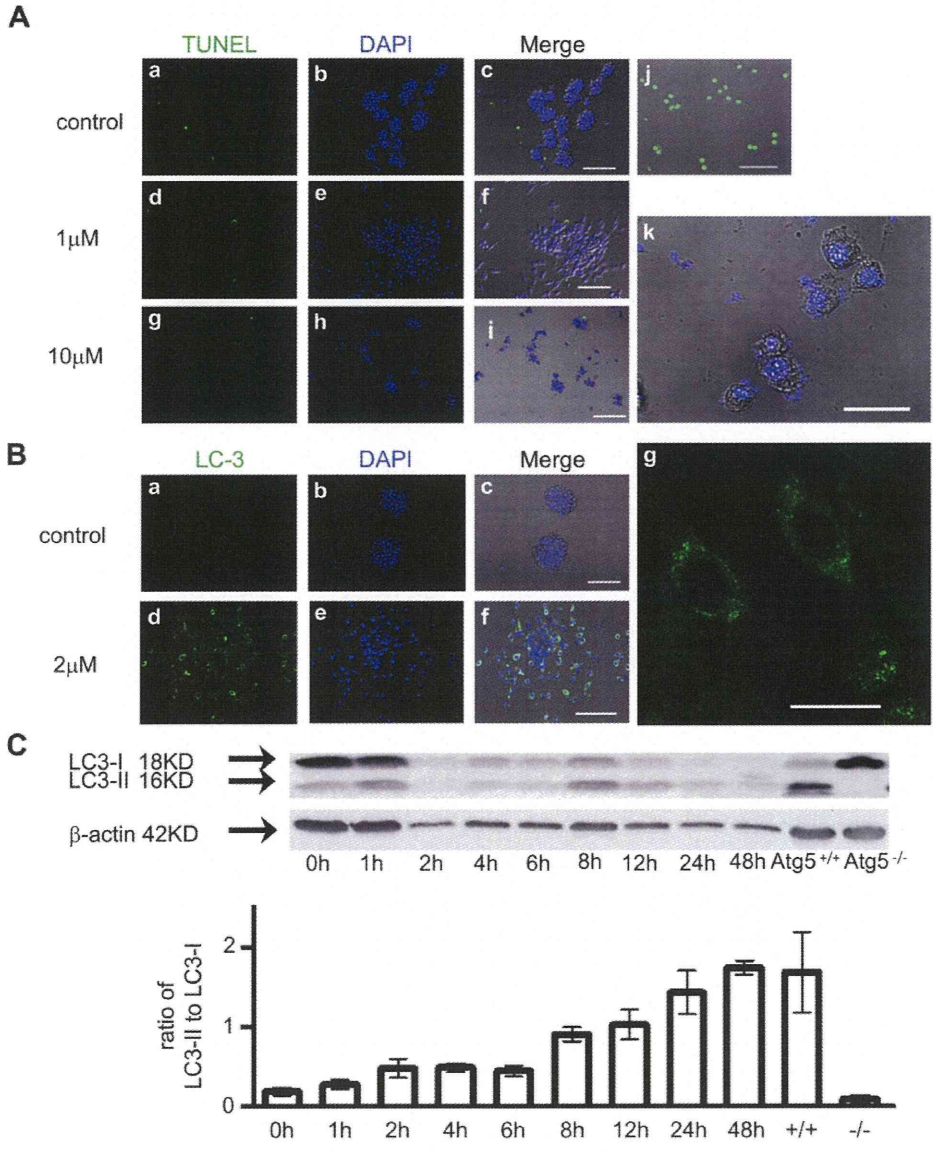

Fig. 3. Induction of autophagy but not apoptosis of GICs with dPasFHV-p53C′. (A) TUNEL staining of GICs treated with 10 μM D-p53C′ peptide (control, a-c), 1 μM dPasFHVp53C′(d–f), and 10 μM (g–i) dPasFHV-p53C′. TUNEL staining was performed 24 h after each peptide application. Nuclei were stained with DAPI (b, e, h and k). For a positive control of TUNEL staining, GICs were treated with 1 mM hydrogen dioxide for 24 h (j). Scale bars, 100 μm (c, f, i and j); 20 μm (k). (B) Immunocytochemical analysis of LC3 in GICs treated with 10 μM D-p53C′ peptide (a–c) and 2 μM dPasFHV-p53C′ (d–f). High magnification view of LC3-positive cells treated with 2 μM dPasFHV-p53C′ (g). Scale bars, 100 μm (c, f); 20 μm (g). (C) Comparison of protein levels between LC3-I and -II. Both protein levels were analyzed by Western blotting with anti-LC3 antibodies. Each protein level was normalized with β-actin. As a control, MEFs lacking *Atg5* (−/−) and possessing wild-type *Atg5* (+/+) were treated with serum-free medium for 24 h. Data are presented as the mean ± S.E.M. n = 4 each.

2.4. TUNEL assay

The TUNEL assay was performed using an *in situ* cell death detection kit (Roche Applied Science, Mannheim, Germany) as described previously [23]. Twenty-four hours after the application of each peptide, cells were fixed with 4% paraformaldehyde dissolved with phosphate-buffered saline (PBS) at 37 °C for 20 min. They were then washed in PBS and treated with 0.1% Triton X-100 at 4 °C for 5 min. After being rinsed, cells were incubated with the TUNEL reaction mixture at 37 °C for 60 min. The nuclei were counter-stained with 4′,6-diamidino-2-phenylindole (DAPI).

2.5. Transmission electron microscopy of autophagosomes in cells

Cells were fixed with 4% paraformaldehyde and 0.1% glutaraldehyde for 60 min at 37 °C. Cells were post-fixed in 1% osmium tetroxide in 0.1 mol/L phosphate buffer (pH 7.4), dehydrated in a graded ethanol series, and flat embedded in Araldite. Ultrathin sections (40–60 nm thick) were placed on grids (200 mesh), and double-stained with uranyl acetate and lead citrate. The sections were observed under an electron microscope (H-7650, Hitachi, Tokyo, Japan).

2.6. Immunocytochemistry

Immunocytochemical staining for Microtubule-associated protein light chain 3 (LC3) was performed using anti-LC3 polyclonal antibody (Medical & Biological Lab., Nagoya, Japan) as described previously [23]. GICs treated with peptide were fixed with 4% paraformaldehyde–PBS at 37 °C for 20 min, washed in PBS, and incubated with 0.1% Triton X-100 at 4 °C for 5 min. The cells were pretreated with 3% BSA in PBS for 30 min at room temperature, and immunostained with the antibody (1:1000) overnight at 4 °C. Images were obtained using a confocal microscope (FV1000, Olympus, Tokyo, Japan).

2.7. Western blotting

Western blotting was performed as described previously [24]. Cells were plated on 6-well dishes 3 days before treatment with each peptide. Cells treated with peptides were lysed with lysis buffer [20 mM HEPES (pH 7.4), 150 mM NaCl, 1 mM EDTA, 1% Triton, 0.2% SDS, and protease inhibitor cocktail (Sigma–Aldrich)]. Protein concentrations were determined using a BCA protein assay kit (Pierce, Rockford, IL), and 50 μg of cell lysate was used for Western blotting. Cell lysates were mixed with loading buffer and boiled for 5 min. The lysates were then separated by SDS-PAGE on a 10% acrylamide gel and transferred to immobilon membranes (Millipore, Bedford, MA). Membranes were blocked for 1 h in 10% skim milk in PBS (pH7.2), and probed overnight with the primary antibodies to detect LC3 (Medical & Biological Lab.), Atg5 (Abcam, Cambridge, UK), and actin (Ab-I, Oncogene Science, Cambridge, MA) as an internal control. Subsequently, membranes were probed with HRP-conjugated secondary antibodies (GE Healthcare Life Sciences, Pittsburgh, PA). Detection was performed using chemiluminescence, according to the manufacturer's recommendations (DuPont, Boston, MA).

2.8. Transfection of siRNA

siRNA oligonucleotides (Nucleic sequences, GAUAUGGUUUGAAUAUGAATT and UUCAUAUUCAAACCAUAUCTT) targeting the Atg5 mRNAs were obtained from Sigma–Aldrich. Transfection of siRNA was performed with Lipofectamine™ RNAiMAX (Invitrogen). An unmodified oligo (44-2926, Invitrogen) was used as a control. GICs seeded on 96-well plates were transfected with siRNA oligonucleotides (50 nM) according to the manufacturer's directions and incubated for 72 h.

2.9. Mouse models of GBM

The mice were obtained from Charles River Laboratories Japan (Yokohama, Japan). All animal procedures were approved by the Animal Ethics Committee of Kumamoto University.

2.9.1. Intracranial transplantation of GICs into the brain of nude mice

Human GICs (1×10^3 cells) were suspended in 3 μl of PBS and injected into the brain of 5- to 8-week-old female nude mice that had been anesthetized with 10% pentobarbital. The stereotactic coordinates of the injection site were 2 mm forward from lambda, 2 mm lateral from the sagittal suture, and 5 mm deep.

2.9.2. Subcutaneous transplantation of GICs

Subcutaneous models were established by injecting 1×10^4 GICs suspended in 3 μl of PBS subcutaneously into the right back of anesthetized nude mice. Tumor size was measured daily using calipers. When the subcutaneous tumor reached ~6.2 mm in diameter, 450 or 45 μg/kg of peptide was injected around the tumor once a day for 5 successive days.

2.10. Statistical analysis

Data are shown as the mean (±S.E.M.). Data were analyzed using either Student's *t* test to compare two conditions or ANOVA followed by planned comparisons of multiple conditions, and $p < 0.05$ was considered to be significant. Survival curves were generated according to the Kaplan-Meijer method, and differences in survival were analyzed by the Wilcoxon rank-sum test. $P < 0.05$ was considered significant.

3. Results

3.1. Efficiency of the delivery of dPasFHV-p53C′-SR101 into human GICs

dPasFHV-p53C′ is delivered effectively into human glioma cells and the peptide has a long-lasting anti-tumor effect [18]. In the present study, it was first examined whether dPasFHV-p53C′ was

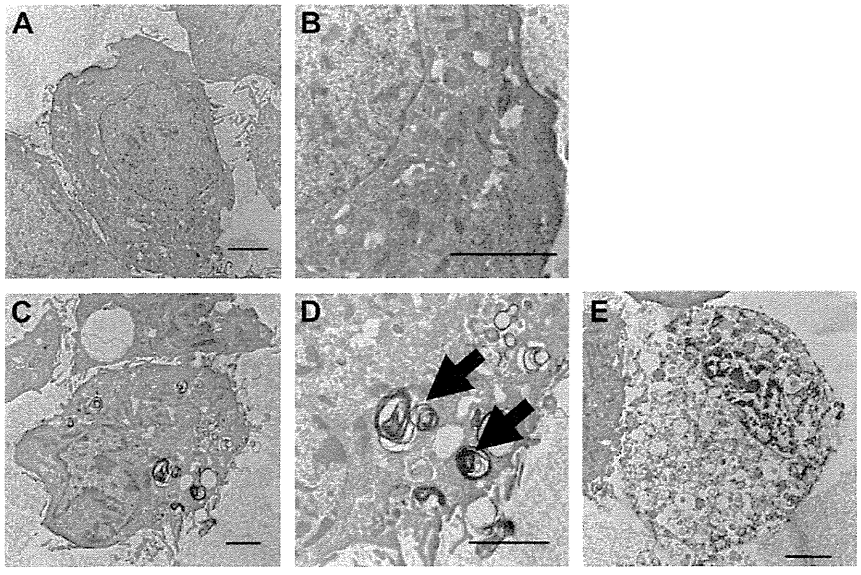

Fig. 4. Electron microscopic analysis of GIC cells treated with 2 μM D-p53C′ (A and B), and 2 μM (C and D) and 10 μM (E) dPasFHV-p53C′ for 24 h. Arrows in D show autophagosomes. Scale bars, 2 μm.

delivered into human GICs. Human GICs were incubated with 10 μM dPasFHV-p53C′-SR101 for 0.5 and 6 h (Fig. 1A). SR101 signals were detected only at the surface of spheres of GICs 0.5 h after the application (Fig. 1Ba–j). However, the signal had diffused into the core of the spheres 6 h after the transduction (Fig. 1Bk–t), suggesting that dPasFHV-p53C′ was effectively delivered in GICs.

3.2. Dose-dependent effect of dPasFHV-p53C′ on the growth of GICs

The dose-dependent effect of dPasFHV-p53C′ on the cell growth of GICs was examined next. The cells were treated with 1, 2, 3, 5, and 10 μM of the peptide for a specific period and the WST-8 assay was performed. D-p53C′ (10 μM) was used as a control. The peptide had no effect at 1 μM, but dose-dependently inhibited growth at more than 2 μM (Fig. 2A,C). At 3 and 5 μM, it almost completely inhibited the growth (Fig. 2A,C). To investigate whether the peptide affects the growth of normal stem cells, mouse embryonic stem (mES) cells were treated with each concentration of dPasFHV-p53C′. Lower concentrations (1–5 μM) of the peptide had no effect whereas 10 μM of the peptide inhibited growth (Fig. 2B,C).

3.3. Observation of autophagy of GICs by dPasFHV-p53C′

We expected dPasFHV-p53C′ to induce the apoptosis of GICs as an effect on glioma cells [18] and examined whether the peptide induced apoptosis with the TUNEL assay. However, 1 and 10 μM peptides did not increase the TUNEL-positive cells although many cells died when treated with 10 μM peptide (Fig. 3A). Moreover, condensed chromatin was not observed in GICs treated with 10 μM peptide (Fig. 3a–k).

Autophagy is a cellular pathway involved in protein and organelle degradation [25] and frequently activated in tumor cells following treatment with chemotherapeutic drugs [26,27] or γ-irradiation [28]. We next examined whether dPasFHV-p53C′ induces the autophagy of GICs. Microtubule-associated protein light chain 3 (LC3) is a marker of autophagosomes. LC3 is processed by Atg4 and becomes LC3-I [29]. Upon the induction of authophagy, the C-terminal glycine of LC3-I is conjugated to phosphatidylethanolamine, resulting in the formation of membrane-bound LC3-II [30]. Most LC3-II is present on the autophagosome membrane [30]. In the present study, LC3 was diffusely and faintly expressed in the cytoplasm of GICs treated with control peptide (Fig. 3Ba–c). In contrast, dense staining of LC3 was observed in the cytoplasm of cells treated with 2 μM peptide for 24 h (Fig. 3Bd-f). Higher magnification revealed the formation of autophagosome vacuoles (green dots) in GICs treated with the peptide (Fig. 3Bg). Protein levels of LC3-II were analyzed with immunoblotting. LC3-II levels increased in a time-dependent manner after treatment with dPasFHV-p53C′ (Fig. 3C). As a control, LC3-II protein levels were increased in $Atg5^{+/+}$ mouse embryonic fibroblasts (MEFs) when incubated in serum-free medium for 24 h whereas LC3-II levels were faint in $Atg5^{-/-}$ MEFs (Fig. 3C).

Electric microscopic analysis revealed double-membraned autophagic vacuoles in the cytoplasm of GICs treated with 2 μM dPasFHV-p53C′ for 24 h (Fig. 4C and D), whereas GICs treated with control peptide didn't exhibit these features (Fig. 4A and B). When GICs were treated with 10 μM dPasFHV-p53C′, much vacuolar degeneration occurred with collapsed autophagosomes seen in the cytoplasm but no condensed chromatin or fragmented nuclei, which are features of apoptosis (Fig. 4E). These results suggest that dPasFHV-p53C′ induced authophagic cell death but not apoptosis of GICs.

3.4. Effect of autophagy on the growth inhibition of GICs by dPasFHV-p53C′

Autophagy is thought to promote the survival of tumor cells in the face of chemotherapeutic drugs and radiation [31]. We next examined whether Inhibition of autophagy induces the inhibitory effect of dPasFHV-p53C′ on the growth of GICs. GICs were treated with siRNA for Atg5, a protein essential to the formation of autophagosomse vesicles, and control siRNA. After 72 h, cells were treated with dPasFHV-p53C′ (day 0) and growth was evaluated with the WST-8 assay. RNAi-mediated knockdown of Atg5 did not affect the growth of GICs (Fig. 5A and B). However, the knockdown induced an inhibitory effect of dPasFHV-p53C′ on the growth when treated with 1 μM of the peptide (Fig. 5A and B).

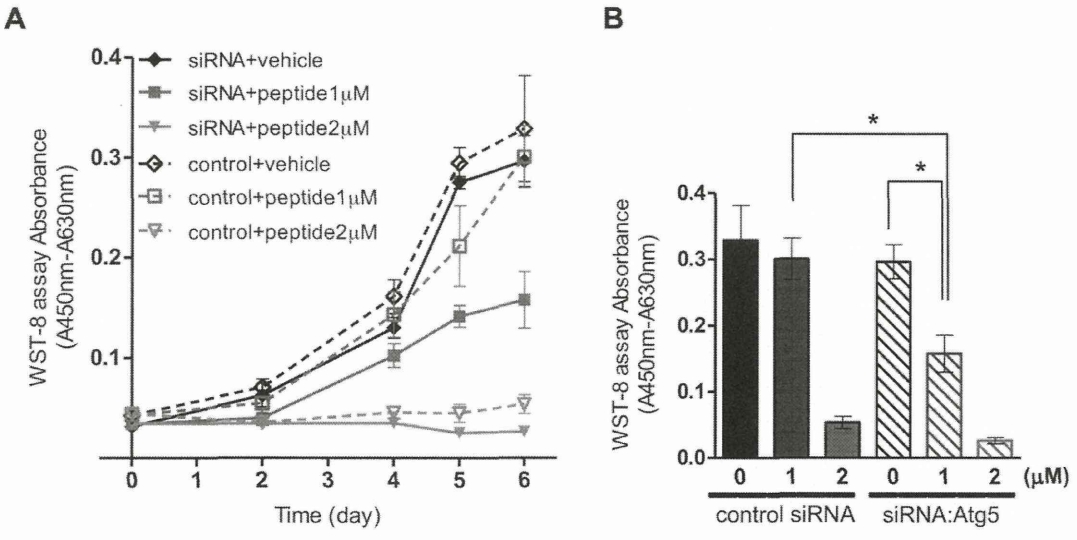

Fig. 5. Effect of knockdown of Atg5 on dPasFHV-p53C′-mediated inhibition of the growth of GICs. (A) GICs were transfected with siRNA of Atg5 (siRNA) and control siRNA (control). After 72 h, cells were treated with 1 and 2 μM dPasFHV-p53C′ (peptide) and vehicle only (vehicle) (day 0). The WST-8 assay was performed every 24 h after the application for 6 successive days. (B). Comparison of the growth at day 6 among each treatment. $n = 8$ each. $^{*}P < 0.001$.

3.5. Effect of dPasFHV on autophagic cell death of GICs

Previous studies have shown that p53C′ induces apoptosis of cancer cells but not autophagic cell death [11,19]. Therefore, p53C′ is unlikely to induce autophagy in GICs. Cancer cells resist chemotherapy and radiation by induction of autophagy [26–28]. For this resistance to be achieved, autophagosomes must fuse with lysosomes [31]. Pas may prevent this because the peptide enhances the translocation of CPPs through endosomal and macropinosomal membranes [18]. We next examined whether dPasFHV without p53C′ induced autophagic cell death of GICs. dPasFHV had no effect on the growth of GICs when applied at 2 μM (Fig. 6A). However, at 3 μM it significantly inhibited, and at 5 μM, completely inhibited the growth (Fig. 6A). The peptides did not induce the apoptosis of GICs the same as dPasFHV-p53C′ (Fig. 6B). When GICs were treated with 2 μM dPasFHV, dense staining of LC3 was observed in the cytoplasm. LC3-II levels also increased after treatment with dPasFHV in a time-dependent manner (Fig. 6C). These results suggest that dPasFHV induces the autophagic cell death of GICs.

3.6. Effect of dPasFHV-p53C′ on survival of tumor-bearing mice and the growth of xenografts of GICs

Finally, we examined the inhibitory effect of dPasFHV-p53C′ on the growth of GICs *in vivo*. The spheres of GICs were dissociated into single cells, and the cells were treated with 1 and 10 μM dPasFHV-p53C′ and 10 μM L-p53C′ (control peptide) for 2 h. GICs (1×10^3 cells) were then transplanted into the brain of nude mice stereotaxically (day 0). GBM formed with human pathological features such as necrotic regions with surrounding pseudopalisades, vascular proliferation, and dividing tumor cells (Supplementary Fig. 1). All of the tumor-bearing mice treated with control peptide developed GBMs and died within 32 days (Fig. 7A). The survival of mice transplanted with GICs treated with 1 μM peptide was slightly prolonged (Fig. 7A). All of the tumor-bearing mice treated with 10 μM peptide survived for 90 days (Fig. 7A).

GICs (1×10^4 cells) were subcutaneously transplanted into nude mice. When the tumor grew to 6.2 mm in diameter about 2 weeks

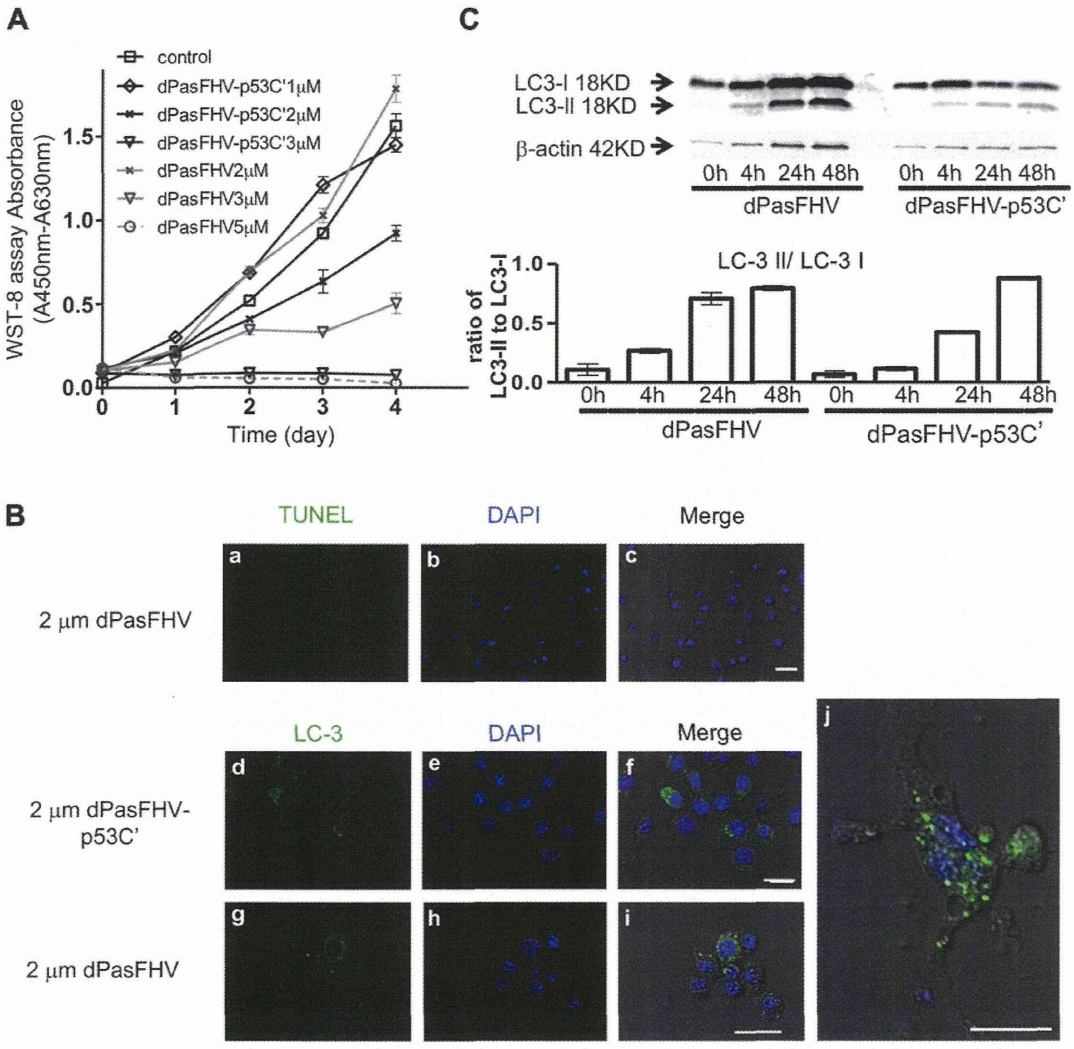

Fig. 6. Effect of dPasFHV on the growth (A) and induction of autophagy (B and C) of GICs. (A) GICs were treated with each concentration of dPasFHV and dPasFHVp53C′. The growth was evaluated with the WST-8 assay. $n = 4$ each. (B) GICs were treated with 2 μM dPasFHV and dPasFHV-p53C′ for 24 h. Cells were then stained with TUNEL (a–c) and immunostained with anti-LC3 antibodies (d–j). (j) High magnification view of LC3-positive cells treated with 2 μM dPasFHV. The nuclei were counterstained with DAPI. Scale bars, 20 μm (c, f and i), 10 μm (j). (C) The protein level of LC3-II increased time-dependently after treatment with 5 μM dPasFHV. Data are presented as the mean ± S.E.M. n = 4 each.

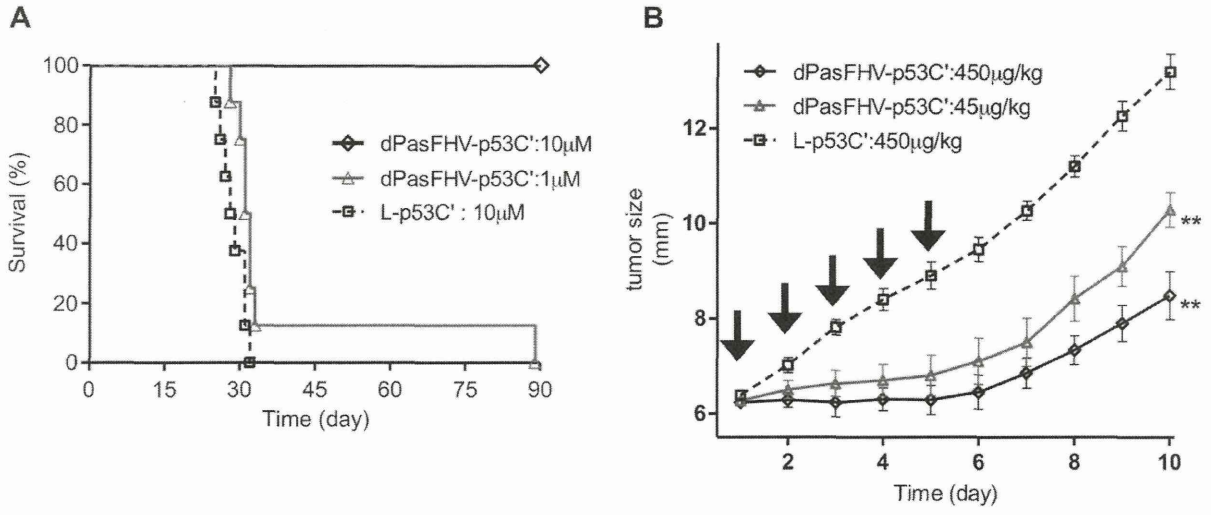

Fig. 7. (A) Effect of dPasFHV-p53C′ on survival rates of nude mice transplanted with GICs (1×10^3) in the brain. Cells were treated with 1 and 10 μM dPasFHV-p53C′, and 10 μM L-p53C′ (control peptide) for 2 h before the transplantation. Nude mice were then transplanted with the cells at day 0. The survival of the mice was measured by monitoring life span and data were analyzed using the Kaplan–Meier method. (B) Effect of dPasFHV-p53C′ on growth of tumors transplanted subcutaneously into nude mice. After a tumor had reached 6.2 mm in diameter, 45 or 450 μg/kg of peptide was injected around it once a day for 5 days. The diameter of the tumor was measured using calipers every 24 h. $n = 6$ each. $^{**}P < 0.001$ vs. control peptide.

after the transplantation, 450 or 45 μg/kg of peptide was injected around the tumor once a day for 5 successive days. L-p53C′ was injected as a control. Tumor growth was completely inhibited until day 6 when treated with 450 μg/kg peptide (Fig. 7B). Tumor size gradually increased after 7 days but was significantly smaller than that of mice treated with control peptide at day 10 (Fig. 7B).

4. Discussion

GBM is characterized by resistance to chemotherapy and radiotherapy. Therefore, the prognosis of patients with GBM remains extremely poor and has not changed significantly during the last decade [32]. CD133-positive GICs have been implicated in the enhanced radiation- and chemotherapy-resistance and in the repopulation of tumors following these treatments [6,33]. New strategies for killing GICs are indispensable to develop anti-GBM therapy. In the present study, we showed that dPasFHV-p53C′ inhibited the growth of GICs in a dose-dependent manner. At 3 μM, the peptide almost completely inhibited the growth of the cells but had no effect on the growth of mouse embryonic stem cells. Moreover, the peptide significantly inhibited the growth of tumors in mice implanted with human GICs. We previously showed that dPasFHV-p53C′ inhibited the growth of human malignant glioma cell lines [18], and induced the apoptosis of bladder cancer cells but had no effect on normal cells [19]. GBM is made up of intermingled glioma cells and GICs. To cure GBM, therefore, it is important to treat both cells. p53C′ induced the apoptosis of cancer cells [19] and Pas induced the autophagic cell death of GICs as shown in the present study. These results suggest that dPasFHV-p53C′ may be promising for GBM therapy.

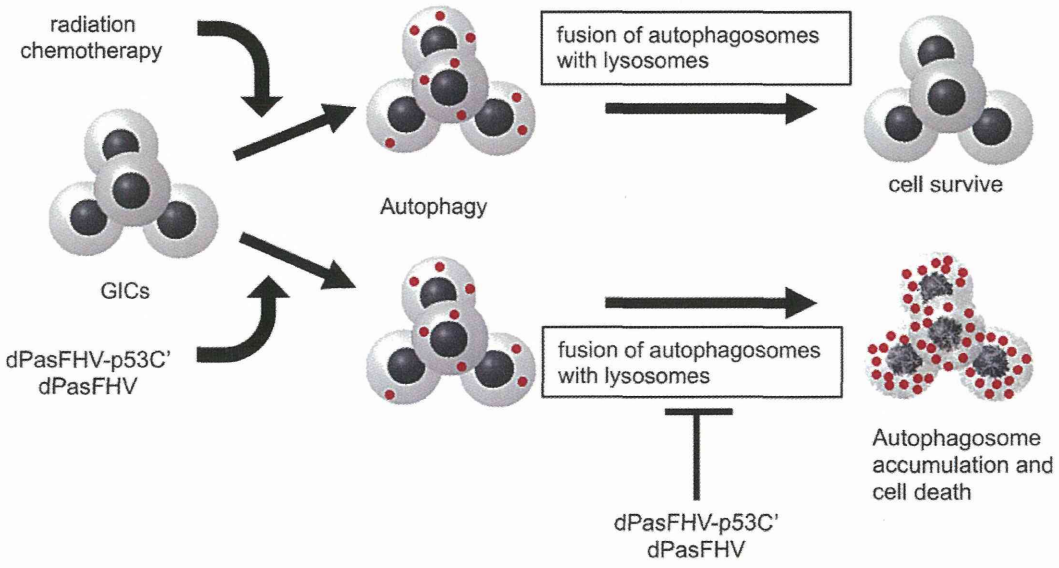

Fig. 8. Scheme of the induction of autophagic cell death of GICs by dPasFHV-p53C′ and dPasFHV.

In the present study, dPasFHV without p53C′ induced the autophagic cell death of GICs, suggestting Pas to play a critical role in the induction of autophagy. Autophagy is a cellular pathway involved in protein and organelle degradation [25] and frequently activated in tumor cells following treatment with chemotherapeutic drugs [26,27] or γ-irradiation [28]. Autophagy is a catabolic process involving the degradation of the components of a cell by its own lysosomal machinery and a major mechanism by which a starving cell reallocates nutrients from unnecessary processes to more essential processes [31]. Recent studies showed that GICs contributes to the radioresistance of GBM with the induction of autophagy [34,35]. The induction of authophagy in GICs treated with dPasFHV-p53C′ may protect against apoptotic cell death. Although GICs are capable of escaping cell death by autophagy when treated with existing chemotherapeutic drugs, cells treated with dPasFHV-p53C′ and dPasFHV showed autophagic cell death. Chloroquine, used for the treatment of malaria, arrests the autophagy pathway by disrupting the cellular lysosomal function and altering the fusion of autophagosomes with lysosomes, resulting in the accumulation of autophagosomes and induction of autophagic cell death [31]. Pas enhances the internalization efficiency of arginine-rich CPPs including poly-arginine and FHV peptides [18]. This effect may be due to the disruption of macropinosomal and endosomal membranes in which cell-penetrating peptides are entrapped and prevention of the subsequent fusion with lysosomes and degradation in lysosomes [18]. These results suggest that dPasFHV may induce autophagic cell death of GICs by preventing the fusion of autophagosomes with lysosomes (Fig. 8).

5. Conclusion

The present results showed that dPasFHV-p53C′ and dPasFHV induced autophagic cell death of GICs. dPasFHV-p53C′ reduced tumor mass in mice transplanted with GICs. The present results suggest peptide transduction therapy using dPasFHV-p53C′ to be a method for the treatment of GBM.

Acknowledgments

We thank N. Maeda for technical assistance. This work was supported by a Grant-in-aid for Scientific Research from the Ministry of Education, Culture, Sports, Science and Technology of Japan and by the Japan Society for the Promotion of Science (JSPS) through its "Funding Program for Next Generation World-Leading Researchers".

Appendix A. Supplementary data

Supplementary data related to this article can be found at http://dx.doi.org/10.1016/j.biomaterials.2012.09.003.

References

[1] Van Meir EG, Hadjipanayis CG, Norden AD, Shu HK, Wen PY, Olson JJ. Exciting new advances in neuro-oncology: the avenue to a cure for malignant glioma. CA Cancer J Clin 2010;60:166–93.
[2] Kohsaka S, Wang L, Yachi K, Mahabir R, Narita T, Itoh T, et al. STAT3 inhibition overcomes temozolomide resistance in glioblastoma by downregulating MGMT expression. Mol Cancer Ther 2012;11:1289–99.
[3] Singh SK, Clarke ID, Hide T, Dirks PB. Cancer stem cells in nervous system tumors. Oncogene 2004;23:7267–73.
[4] Singh SK, Clarke ID, Terasaki M, Bonn VE, Hawkins C, Squire J, et al. Identification of a cancer stem cell in human brain tumors. Cancer Res 2003;63:5821–8.
[5] Singh SK, Hawkins C, Clarke ID, Squire JA, Bayani J, Hide T, et al. Identification of human brain tumor initiating cells. Nature 2004;432:396–401.
[6] Beier H, Hau P, Proescholdt M, Lohmeier A, Wischhusen J, Oefner PJ, et al. CD133(+) and CD133(-) glioblastoma-derived cancer stem cells show differential growth characteristics and molecular profiles. Cancer Res 2007;67:4010–5.
[7] Eyler CE, Rich JN. Survival of the fittest: cancer stem cells in therapeutic resistance and angiogenesis. J Clin Oncol 2008;26:2839–45.
[8] Bode AM, Dong Z. Post-translational modification of p53 in tumorigenesis. Nat Rev Cancer 2004;4:793–805.
[9] Olsson A, Manzl C, Strasser A, Villunger A. How important are post-translational modifications in p53 for selectivity in target-gene transcription and tumor suppression? Cell Death Differ 2007;14:1561–75.
[10] Hupp TR, Sparks A, Lane DP. Small peptides activate the latent sequence-specific DNA binding function of p53. Cell 1995;83:237–45.
[11] Snyder EL, Meade BR, Saenz CC, Dowdy SF. Treatment of terminal peritoneal carcinomatosis by a transducible p53-activating peptide. PLoS Biol 2004;2:E36.
[12] Joliot A, Prochiantz A. Transduction peptides: from technology to physiology. Nat Cell Biol 2004;6:189–96.
[13] Gupta B, Levchenko TS, Torchilin VP. Intracellular delivery of large molecules and small particles by cell-penetrating proteins and peptides. Adv Drug Deliv Rev 2005;57:637–51.
[14] Wadia JS, Dowdy SF. Transmembrane delivery of protein and peptide drugs by TAT-mediated transduction in the treatment of cancer. Adv Drug Deliv Rev 2005;57:579–96.
[15] Snyder EL, Saenz CC, Denicourt C, Meade BR, Cui XS, Kaplan IM, et al. Enhanced targeting and killing of tumor cells expressing the CXC chemokine receptor 4 by transducible anticancer peptides. Cancer Res 2005;65:10646–50.
[16] Wadia JS, Stan RV, Dowdy SF. Transducible TAT-HA fusogenic peptide enhances escape of TAT-fusion proteins after lipid raft macropinocytosis. Nat Med 2004;10:310–5.
[17] Yasuda Y, Kageyama T, Akamine A, Shibata M, Kominami E, Uchiyama Y, et al. Characterization of new fluorogenic substrates for the rapid and sensitive assay of cathepsin E and cathepsin D. J Biochem 1999;125:1137–43.
[18] Takayama K, Nakase I, Michiue H, Takeuchi T, Tomizawa K, Matsui H, et al. Enhanced intracellular delivery using arginine-rich peptides by the addition of penetration accelerating sequences (Pas). J Control Release 2009;138:128–33.
[19] Araki D, Takayama K, Inoue M, Watanabe T, Kumon H, Futaki S, et al. Cell-penetrating D-isomer peptides of p53 C-terminus: long-term inhibitory effect on the growth of bladder cancer. Urology 2010;75:813–9.
[20] Takezaki T, Hide T, Takanaga H, Nakamura H, Kuratsu J, Kondo T. Essential role of the Hedgehog signaling pathway in human glioma-initiating cells. Cancer Sci 2011;102:1306–12.
[21] Kondo T. Brain cancer stem-like cells. Eur J Cancer 2006;42:1237–42.
[22] Higuchi Y, Shiraki N, Yamane K, Qin Z, Mochitate K, Araki K, et al. Synthesized basement membranes direct the differentiation of mouse embryonic stem cells into pancreatic lineages. J Cell Sci 2010;123:2733–42.
[23] Wu HY, Tomizawa K, Oda Y, Wei FY, Lu YF, Matsushita M, et al. Critical role of calpain-mediated cleavage of calcineurin in excitotoxic neurodegeneration. J Biol Chem 2004;279:4929–40.
[24] Tomizawa K, Sunada S, Lu YF, Oda Y, Kinuta M, Ohshima T, et al. Cophosphorylation of amphiphysin I and dynamin I by Cdk5 regulates clathrin-mediated endocytosis of synaptic vesicles. J Cell Biol 2003;163:813–24.
[25] Klionsky DJ, Emr SD. Autophagy as a regulated pathway of cellular degradation. Science 2000;290:1717–21.
[26] Kim EH, Sohn S, Kwon HJ, Kim SU, Kim MJ, Lee SJ, et al. Sodium selenite induces superoxide-mediated mitochondrial damage and subsequent autophagic cell death in malignant glioma cells. Cancer Res 2007;67:6314–24.
[27] Abedin MJ, Wang D, McDonnell MA, Lehmann U, Kelekar A. Autophagy delays apoptotic death in breast cancer cells following DNA damage. Cell Death Differ 2007;14:500–10.
[28] Apel A, Herr I, Schwarz H, Rodemann HP, Mayer A. Blocked autophagy sensitizes resistant carcinoma cells to radiation therapy. Cancer Res 2008;68:1485–94.
[29] Kabeya Y, Mizushima N, Ueno T, Yamamoto A, Kirisako T, Noda T, et al. LC3, a mammalian homologue of yeast Apg8p, is localized in autophagosome membranes after processing. EMBO J 2000;19:5720–8.
[30] Mizushima N, Yoshimori T. How to interpret LC3 immunoblotting. Autophagy 2007;3:542–5.
[31] Espina V, Liotta LA. What is the malignant nature of human ductal carcinoma in situ? Nat Rev Cancer 2011;11:68–75.
[32] Maher EA, Furnari FB, Bachoo RM, Rowitch DH, Louis DN, Cavenee WK, et al. Malignant glioma: genetics and biology of a grave matter. Genes Dev 2001;15:1311–33.
[33] Bao S, Wu Q, McLendon RE, Hao Y, Shi Q, Hjelmeland AB, et al. Glioma stem cells promote radioresistance by preferential activation of the DNA damage response. Nature 2006;444:756–60.
[34] Lomonaco SL, Finniss S, Xiang C, Decarvalho A, Umansky F, Kalkanis SN, et al. The induction of autophagy by gamma-radiation contributes to the radioresistance of glioma stem cells. Int J Cancer 2009;125:717–22.
[35] Lomonaco SL, Finniss S, Xiang C, Lee HK, Jiang W, Lemke N, et al. Cilengitide induces autophagy-mediated cell death in glioma cells. Neuro Oncol 2011;13:857–65.

THE JOURNAL OF BIOLOGICAL CHEMISTRY VOL. 287, NO. 27, pp. 23236–23245, June 29, 2012
Published in the U.S.A.

Anks4b, a Novel Target of HNF4α Protein, Interacts with GRP78 Protein and Regulates Endoplasmic Reticulum Stress-induced Apoptosis in Pancreatic β-Cells*[S]

Received for publication, April 3, 2012, and in revised form, May 11, 2012 Published, JBC Papers in Press, May 15, 2012, DOI 10.1074/jbc.M112.368779

Yoshifumi Sato[‡1], Mitsutoki Hatta[‡1], Md. Fazlul Karim[‡1,2], Tomohiro Sawa[§¶], Fan-Yan Wei[‖], Shoki Sato[‡], Mark A. Magnuson[**], Frank J. Gonzalez[‡‡], Kazuhito Tomizawa[‖], Takaaki Akaike[§], Tatsuya Yoshizawa[‡], and Kazuya Yamagata[‡3]

From the Departments of [‡]Medical Biochemistry and [§]Microbiology, Faculty of Life Sciences, Kumamoto University, Kumamoto 860-8556, Japan, [¶]PRESTO, Japan Science and Technology Agency (JST), 4-1-8 Honcho Kawaguchi, Saitama 332-001, Japan, the [‖]Department of Molecular Physiology, Faculty of Life Sciences, Kumamoto University, Kumamoto, Japan the [**]Department of Molecular Physiology and Biophysics, Vanderbilt University School of Medicine, Nashville, Tennessee 37232, and the [‡‡]Laboratory of Metabolism, NCI, National Institutes of Health, Bethesda, Maryland 20814

Background: Target genes of HNF4α in β-cells are largely unknown.
Results: Expression of Anks4b is decreased in the βHNF4α KO islets. HNF4α activates Anks4b promoter activity. Anks4b binds to GRP78 and regulates sensitivity to ER stress.
Conclusion: HNF4α novel target gene, *Anks4b*, regulates the susceptibility of β-cells to ER stress.
Significance: Anks4b is a novel molecule involved in ER stress.

Mutations of the *HNF4A* gene cause a form of maturity-onset diabetes of the young (MODY1) that is characterized by impairment of pancreatic β-cell function. HNF4α is a transcription factor belonging to the nuclear receptor superfamily (NR2A1), but its target genes in pancreatic β-cells are largely unknown. Here, we report that ankyrin repeat and sterile α motif domain containing 4b (Anks4b) is a target of HNF4α in pancreatic β-cells. Expression of Anks4b was decreased in both βHNF4α KO islets and HNF4α knockdown MIN6 β-cells, and HNF4α activated Anks4b promoter activity. Anks4b bound to glucose-regulated protein 78 (GRP78), a major endoplasmic reticulum (ER) chaperone protein, and overexpression of Anks4b enhanced the ER stress response and ER stress-associated apoptosis of MIN6 cells. Conversely, suppression of Anks4b reduced β-cell susceptibility to ER stress-induced apoptosis. These results indicate that Anks4b is a HNF4α target gene that regulates ER stress in β-cells by interacting with GRP78, thus suggesting that HNF4α is involved in maintenance of the ER.

Hepatocyte nuclear factor (HNF)[4] 4α, a transcription factor belonging to the nuclear receptor superfamily (NR2A1), is expressed in the liver, pancreas, kidney, and intestine (1, 2). HNF4α has multiple functional domains, including the N-terminal A/B domain associated with the transactivation domain (AF-1), a DNA binding C domain, a functionally complex E domain that forms a ligand binding domain, a dimerization interface and transactivation domain (AF-2), and an F domain with a negative regulatory function (3, 4). HNF4α predominantly binds to a 6-bp repeat (AGGTCA) with a 1-bp spacer (mainly A) called direct repeat (DR1).

Maturity-onset diabetes of the young (MODY) is a genetically heterogeneous monogenic disorder that accounts for 2–5% of type 2 diabetes (5). We discovered that mutations of the human *HNF4A* gene cause a particular form of MODY known as MODY1 (6). The primary pathogenesis of MODY1 involves dysfunction of pancreatic β-cells (5). In addition, it has been shown that targeted disruption of HNF4α in pancreatic β-cells leads to defective insulin secretion in mice (7, 8). These findings have demonstrated that HNF4α has an important role in β-cells.

In the liver, HNF4α plays a critical role in nutrient transport and metabolism by regulating numerous target genes, including phosphoenolpyruvate carboxykinase (*PCK1*), glucose-6-phosphatase (*G6PC*), apolipoprotein AII (*APOA2*), and microsomal triglyceride transfer protein (*MTTP*) (9, 10). In contrast, we have little information about the target genes of HNF4α in pancreatic β-cells. Previous *in vitro* studies have suggested that

* This work was supported by a grant-in-aid for scientific research (B), a grant-in-aid for scientific research (S), a grant-in-aid for scientific research in innovative areas, a grant from the Ministry of Health Labour and Welfare, a grant from Takeda Science Foundation, a grant from Novo Nordisk Insulin Research Foundation, a grant from Banyu Life Science Foundation International, and a grant from Japan Diabetes Foundation.
[S] This article contains supplemental Tables 1 and 2 and supplemental Figs. 1–8.
[1] These authors contributed equally to this work.
[2] Supported by a scholarship from the International Priority Graduate Programs Advanced Graduate Courses for International Students, Ministry of Education, Culture, Sports, Science, and Technology in Japan.
[3] To whom correspondence should be addressed. Fax: 81-96-364-6940; E-mail: k-yamaga@kumamoto-u.ac.jp.

[4] The abbreviations used are: HNF, hepatocyte nuclear factor; MODY, Maturity-onset diabetes of the young; ER, endoplasmic reticulum; Anks4b, ankyrin repeat and sterile α motif domain containing 4b; TG, thapsigargin; CHOP, C/EBP homologous protein; C/EBP, CCAAT-enhancer-binding protein; BiP, binding immunoglobulin protein; ESI-Q-TOF, electrospray mass ionization-quadrupole-time-of-flight; KD, knockdown; FL, full-length; MUT, mutant.

HNF4α regulates the expression of pancreatic β-cell genes involved in glucose metabolism, such as insulin (*INS*), solute carrier family 2 (*SLC2A2*), and *HNF1A* (11). However, the expression of these genes was unchanged in the islets of β-cell-specific HNF4α knock-out (βHNF4α KO) mice (7, 8), indicating that such genes are not targets of HNF4α *in vivo*, at least in β-cells.

In the present study, we investigated the mRNA expression profile of βHNF4α KO mice and found that ankyrin repeat and sterile α motif domain containing 4b/harmonin-interacting, ankyrin repeat-containing protein (Anks4b/Harp) is a target of HNF4α in β-cells. We also demonstrated that Anks4b interacts with glucose-regulated protein 78 (GRP78), a major chaperone protein that protects cells from endoplasmic reticulum (ER) stress *in vitro* and *in vivo*. Gain- and loss-of-function studies of Anks4b revealed that it regulates sensitivity to thapsigargin (TG)-induced ER stress and apoptosis in MIN6 β-cell line. Our results suggest that HNF4α plays an important role in the regulation of ER stress and apoptosis in pancreatic β-cells.

EXPERIMENTAL PROCEDURES

Microarray Expression Profiling and HNF4α Motif Scan—Mice were maintained on a 12-h light/12-h dark cycle and allowed free access to food and water. All animal experiments were conducted according to the guidelines of the Institutional Animal Committee of Kumamoto University. Pancreatic islets were isolated from 45-week-old female βHNF4α KO mice ($n = 5$) and control flox/flox mice ($n = 5$) by collagenase digestion (12). Total RNA was prepared from the isolated islets with an RNeasy micro kit (Qiagen) according to the manufacturer's instructions, and its quality was confirmed by using an Agilent 2100 Bioanalyzer (Agilent Technologies, Palo Alto, CA). DNA microarray analysis was performed by the Kurabo GeneChip custom analysis service with GeneChip mouse genome 430 2.0 array (Affymetrix Inc., Santa Clara, CA). For identification of potential HNF4α binding sites, 5 kb of the promoter sequence upstream of the transcriptional start site was retrieved from the University of California Santa Cruz Genome Browser, and the sequence was analyzed by using the Transcription Element Search System (TESS) and the HNF4 Motif Finder generated by Sladek and colleagues (38).

Quantitative RT-PCR—Total RNA was extracted using an RNeasy micro kit (catalog number 74004, Qiagen, Valencia, CA) or Sepasol-RNA I super reagent (Nacalai Tesque, Kyoto, Japan). Then 1 μg of total RNA was used to synthesize first-strand cDNA with a PrimeScript RT reagent kit and gDNA Eraser (RR047A, TaKaRa Bio Inc., Shiga, Japan) according to the manufacturer's instructions. Quantitative real-time PCR was performed using SYBR *Premix Ex Taq* II (RR820A, TaKaRa) in an ABI 7300 thermal cycler (Applied Biosystems, Foster City, CA). The specific primers employed are shown in supplemental Table 1. Relative expression of each gene was normalized to that of TATA-binding protein.

Cell Lines and Culture—The MIN6 pancreatic β-cell line was cultured in Dulbecco's modified Eagle's medium (DMEM) containing 25 mM glucose, 15% fetal bovine serum, 0.1% penicillin/streptomycin, and 50 μM 2-mercaptoethanol at 37 °C under 5% CO_2, 95% air (13). HEK293, HeLa, and COS-7 cells were purchased from the American Type Culture Collection (ATCC) and were cultured in DMEM containing 2.5 mM glucose, 10% fetal bovine serum, and 0.02% penicillin/streptomycin.

Western Blotting—Cells were lysed in radioimmunoprecipitation assay buffer (50 mM Tris-HCl (pH 8.0), 150 mM NaCl, 0.1% SDS, 1% Nonidet P-40, 5 mM EDTA, 0.5% sodium deoxycholate, 20 μg/ml Na_3VO_4, 10 mM NaF, 1 mM PMSF, 2 mM DTT, and protease inhibitor mixture (1/100)) from Nacalai Tesque. Total protein was separated by SDS-polyacrylamide gel electrophoresis, transferred to a polyvinylidene fluoride (PVDF) membrane (Immobilon-P; Millipore, Bedford, MA), and probed with primary antibodies. After incubation with the secondary antibodies, the proteins were visualized using Chemi-Lumi One Super (Nacalai Tesque) and a LAS-1000 imaging system (Fuji Film, Tokyo, Japan). The primary antibodies used in this study were as follows: anti-HNF4α (1:1000) (H1415; Perseus Proteomics, Tokyo, Japan), anti-β-actin (1:2000) (A5441; Sigma-Aldrich), anti-harmonin (SAB250188; Sigma-Aldrich) (1:1000), anti-cleaved caspase-3 (Asp-175) (1:1000) (antibody 9661, Cell Signaling), and anti-GRP78 (1:1000) (sc-1051, Santa Cruz Biotechnology or antibody 4332, Cell Signaling).

Anti-Anks4b antiserum was generated by using a peptide that formed the central region of mouse Anks4b protein (amino acid residues 147–344). The nucleotide sequence of the peptide was amplified by PCR using a pair of primers (5′-CGGATCCCCATGAAAGAGTGCGAACGGCTT-3′ and 5′-CGGATCCCCTTACCATTCTACTTCTTCTTC-3′), and then it was subcloned into the pET28C+ vector. After expression in *Escherichia coli* BL21 (DE3), the His-tagged peptide was purified with His binding resin (Novagen) according to the manufacturer's instructions and dialyzed in a buffer containing 20 mM Tris-HCl (pH 8.0) and 500 mM NaCl. Subsequently, this peptide was used to inoculate rabbits for the production of anti-Anks4b antiserum.

Transient Transfection and Luciferase Reporter Assay—The mouse Anks4b promoter containing a putative HNF4α binding site was amplified by PCR using a pair of primers (5′-AGTGGTCATTGCCATGGTTGGT-3′ and 5′-AGGTAGGAGTCTTTGTCTAGGC-3′), and then it was subcloned into the pGL3 basic reporter (Promega). Transcription binding sites were altered by PCR-based mutagenesis to produce an HNF4α binding site mutant (GAACGGGGGCC) and an HNF1α binding site mutant (CTGACCGGCCAG). CD1b-HNF4α is a dominant negative mutant of HNF4α lacking the AF-2 activation domain (3). As described previously (14), the CD1b mutation was introduced by PCR into pcDNA3-HNF4α7 (kindly provided by Dr. Toshiya Tanaka, Tokyo University). The pcDNA3.1-wild-type (WT)-HNF1α and pcDNA3.1-P291fsinsC-HNF1α expression plasmids have been described previously (15). MIN6 cells or HEK293 cells (3×10^5 cells each) were seeded into 24-well plates at 18 h before transfection. Transient transfection was performed using Lipofectamine 2000 (Invitrogen) or X-treme GENE (Roche Applied Science) according to the manufacturer's instructions. At 24 h after transfection, luciferase activity was measured by using a Dual-Luciferase reporter assay system (Promega).